Steps Towards the Virtual Tower:
Remote Airport Traffic Control Center (RAiCe)

N. Fürstenau, M. Schmidt, M. Rudolph, C. Möhlenbrink, A. Papenfuß, and S. Kaltenhäuser

*Institute of Flight Guidance
German Aerospace Center (DLR)
Braunschweig, Germany
norbert.fuerstenau@dlr.de

Abstract: In this paper research is described which aims at the long term goal of a Virtual Airport Tower without the need of a real tower building, however with improved functionality. Specifically we address the intermediate step of a Remote Airport Tower Center (RTC) for remote surveillance and control of small airports. Because previous work and task analyses indicated the importance of the visual information for present days controller's work procedures, an experimental high resolution video panorama system was developed as main HMI. Field tests of the reconstructed far view yield the effective visual resolution of a 180°-video panorama in agreement with the theoretical predictions. The digital video panorama provides the framework for video-see-through augmented vision by integration of additional information like weather and transponder data, and it allows for panorama replay. An integrated zoom function provides a "foveal" component by means of a remotely controlled pan-tilt zoom camera, including object tracking options, with a high resolution exceeding the human eye within an observation angle < 15°. Simulation environments are under development, based on a two-airport tower-simulator and a Petri-net based computer simulation using a simplified airport microworld. They support design of the new work environment and safety analysis.

Keywords: Virtual tower, remote tower center, panorama display, zoom, augmented vision, resolution, simulation

1. INTRODUCTION

Anticipating the future growth of air traffic and the framework defined by programs as SESAR, Vision 2020 or NextGen a need for Remote Control Centers already exists and will become more urgent in the near future [17[18]]. Furthermore discussions and workshops with stakeholders during previous Virtual and Remote Tower projects (e.g. [19]) identified the need of stakeholders for concepts and solutions for Remote Tower Centers (RTC).

Remote Airport traffic Control Center (RAiCe) describes the goal of providing aerodrome control service for several small airports from a remotely located control center (RTC) without direct far view to the airport surface. Because small airfields usually lack any advanced electronic surveillance system a high resolution augmented vision video panorama as a potential low cost system was proposed to replace the direct far view out of the tower windows as main component of the Human Machine Interface (HMI) [1][2]. RTC is realised within the DLR project RAiCe as intermediate step towards the Virtual Tower as long term goal.

A number of tower work analyses performed during the recent years determined the importance of visual surveillance of the tower and apron controllers for creating their situational awareness, despite the availability of electronic surveillance [3][4][6][14]. In the tower environment of large airports the permanent refocusing between far view and displays contributes to workload and increases head-down time [4]. Both

may be reduced by a high resolution panorama display in a distance to the operator comparable to radar and flight data displays. Consequently it is assumed that under the guideline of human centered automation, the reconstruction of the far view from the control tower of small airports will improve the transition process to a towerless work environment and make it acceptable to the remote Tower Operation (RTO) controller.

Within the previous DLR project "RapTOr" (Remote Airport Tower Operation Research) an RTO experimental system was realized at the Braunschweig research airport BWE [1][2][14][15]. Research was accompanied by a structured work and task analysis [5][6] and model based simulations of controller's decision processes [8]. An experimental 180° video panorama system was developed as core of the RTO controller's HMI. For designing a compact RTO work environment video see-through augmented tower vision (ATV) was realized by integrating information from real time image processing and electronic surveillance sensors like multilateration into the digital videopanorama. ATV was proposed by several authors before, however aiming at augmenting the real far view by means of optical see through head mounted [20] and head up displays, e.g.[11][12] which involve the problem of latency between real world changes and coherently superimposed information and of visual instabilities[13]. This is avoided with the present approach.

Section 2 introduces the basic RTC HMI concept for two alternative airport traffic scenarios. Section 3 describes the augmented vision video panorama system

as basis of the experimental RTC. Results of field trials are reported in section 4. In section 5 simulation environments are described which will be used for supporting HMI and RTC-work system design. Development of a two-airport RTC-tower simulator as well as model based computer simulation are outlined. Section 6 provides a conclusion and outlook.

2. REMOTE TOWER CENTER SCENARIOS

Within RAiCe different RTC configurations and processes for work organisation will be designed and validated. Therefore a set of scenarios regarding sensor equipment, traffic management and work organization is defined. The specific configuration of a center depends on the specific local traffic situation, for which the centre has to cater. Nevertheless the new working environment and structure has to assure that air traffic can be managed safely and efficiently.

As a first step two basic scenarios for remote control center configurations have been chosen. They will be used for experimentation and validation; therefore they are implemented as a part task simulation microworld and as a high fidelity simulation. This is described in more detail in section 5.

In the first scenario a small local airport is controlled from the tower of a larger airport. Because a regional airport by definition has less IFR than VFR traffic an improved more efficient kind of work distribution between (tower, ground, RTO) controllers can be imagined and will be investigated within high fidelity simulation environments as well as microworld computer simulations (see sect. 5). To operationally realize this scenario the compact RTO console would be integrated in the tower of the larger airport.

In the second scenario two small airports will be controlled out of a remote tower center (RTC). The center has to be located in a suitable area, taking into account to be conveniently accessible by the controllers and to provide for the high bandwidth data transmission connections required for the high resolution visual information with 20 – 25 Hz framerate.

On top of these basic traffic scenarios further scenarios regarding the sensor equipment, work organization and further automation support will be investigated.

3. EXPERIMENTAL VIDEOPANORAMA SYSTEM

In this section the setup of the experimental RTO system at Braunschweig research airport is reviewed [1][2][14].

3.1 Reconstruction of the Far View

Motivated by the above mentioned relevance of visual information for tower work processes, a high resolution video panorama system was set up at Brauschweig research airport.

It serves as experimental environment for investigation of different aspects of the Remote Tower Center concept and development of a demonstrator [1][2][14].

A block diagram of the augmented vision video panorama system is depicted in Figure 1. The sensor component consists of four high resolution (1600 x 1200 pixels) high dynamic range (14 bit/pixel) CCD cameras ($P_{1, 2, 3, 4}$) covering the Braunschweig airport within 180° and a remotely controlled pan-tilt zoom camera (P_5: PTZ).
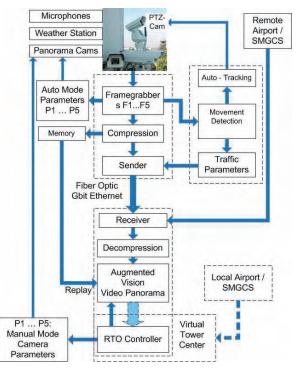

Fig. 1: Schematic block diagram of augmented vision video panorama system. Wide light arrow indicates visual information for the controller.

The cameras (photo in Fig.1) are positioned ca. 20 m above the airport surface, horizontally aligned on top of a building at the southern boundary of the airport with 100 m distance to Braunschweig tower, 400 m south of the runway 08/26 (1670 m). The vertical aperture angle of about 20° (half angle with respect to the horizontal line of sight) allows for a closest surveillance distance of about 60 m. For each camera the signals with 25 frames/s are split into two outputs. One feeds the data compression and encryption (AES256) for transmission to the RTO HMI, while the other drives the simultaneous real time image processing running on a parallel workstation. Figure 2 shows an aerial view of the Braunschweig research airport indicating camera position and camera viewing sectors.

A GBit ethernet switch feeds the images from the five sensors into a single mode fiber optic data link which transfers the typically 100 MBit/s data (night-day

average) of the panorama system and PTZ over a distance of 450 m to the visualisation system. A second GBit ethernet switch splits the incoming data into five output channels for decompression with one PC per camera. The PCs also synchronize the displays of the four segments. Each camera is remotely controlled with respect to aperture and γ correction. The PTZ camera is controlled with respect to azimuth, vertical angle and zoom (Z = 1 - 23-fold, focal width 3.6 mm – 82.8 mm, corresponding to 54° - 2.5° visual angle). An overall latency time between image acquisition and panorama visualization of 230 ms – 270 ms was measured by means of a special shuttered laser arrangement.

Fig. 2: Braunschweig research airport BWE with 1.67 km runway 08/26 extending E-W, fiber optic data link (thin yellow lines) connecting sensor containers. Circle with radiating lines indicate panorama camera position and sectors respectively.(Photo: DLR)

The Augmented Vision Videopanorama (AVP-) HMI for a single operator / single airport surveillance in its initial version is based on four 21"-LCD-monitors (UXGA, 1600x1200 Pixels) for displaying the reconstructed panorama and a separate one for display of the remotely controlled PTZ-camera [14][15].

The latest version (Fig.3) is a backprojection system using a selfmade compact construction with beamers projecting onto 31", with 1400x1050 pixels, 3500 ANSI lm, and contrast 3000:1).

Interaction of the operator with the panorama system (cameras, weather station, microphone) is performed via pen touch-input display. For PTZ positioning the target can be defined manually or by automatic movement detection. A rectangular contour is positioned at the respective location of the panorama, defining the target area to be enlarged. With the tracking mode turned on the square moves coherently with the corresponding object. An algorithm for real time movement detection is running on a separate parallel processor of the image compression PCs of each camera.

The five recording PC's with the compression software at the camera position allow for storing panorama and

zoom data (roughly 500 GByte of data per day) and provide the possibility of complete panorama replay.

In order to obtain a compact RTO HMI which should fit into a typical tower environment of a larger airport, one of the pen touch-input displays in the console of Fig. 3 is designed to incorporate video panorama control features as well as traffic information, e.g. electronic flight strips. A mini-panorama at the top is updated with 1 Hz and serves for commanding the PTZ camera orientation via pointing of the touch-pen. The display also contains buttons for optical PTZ-parameters and activation of automatic object tracking via movement detection, a virtual joystic as an additional option for PTZ orientation, and weather data. For minimizing the number of additional interaction systems and displays integration of relevant traffic information into the videopanorama by using augmented vision techniques is one of the design goals.

Fig. 3: RTO HMI for 180° single airport surveillance, integrating videopanorama. Backprojection displays for cameras no. 1=W – 4= E, PTZ display below (right), and pen touch-input interaction display (left) integrated in the table.(Photo: DLR)

3.2 Augmented Vision

Within the video panorama real-time aircraft position information is integrated as obtained from the multilateration system at the Braunschweig airport via the aircraft (a/c) transponder. An example is shown in Fig. 4 where in display no.4 (E) a yellow transponder code with multilateration position is shown.

It indicates a/c position on the approach glide path. Under reduced visibility this Augmented Tower Vision (ATV) feature allows for localizing the a/c near the correct position because the transponder code, a/c label and numerical information are integrated near the nominal a/c image location in real time.

Another example of augmented vision data is the integration of GPS-position information transmitted via ADS-B. An example is shown in Fig. 4 where D-GPS data measured during flight testing (see sect. 4) are superimposed on the video in the form of flight trajectories (red)which, after geo-referencing are

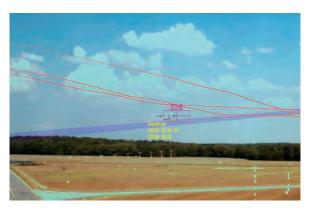transformed from geographical into display coordinates.

Fig. 4: Screenshot of camera no. 4 (= E) display showing augmentation during landing. Superimposed glide path (violett), GPS-trajectories (red), multilateration position (yellow, from transponder) and automatic movement detection (red square).

Contours of the movement areas are superimposed on the reconstructed panorama for guiding the operators attention during low visibility to those areas where moving vehicles are expected. Movement areas are also the preferred targets of a high resolution (640x512) infrared camera system with PTZ function operating in the mid-IR range (2-5 μm) which is presently integrated in the experimental system for improving night vision and visibility under CAT I conditions.

One important advantage of the so called video see-through augmented vision technique using the digital video panorama is the easy integration of augmented vision features. This characteristic avoids the problem of (computational) delay between real scene and augmented information of the optical see-through technology as realized with the head–up and head mounted techniques [11][12][20]. Initial laboratory experiments and theoretical investigations with superimposed information on the far view addressed the human performance such as response time and head down time reduction [4] by using transparent displays for reducing the number of monitors [11][12], and the problem of uncontrolled perceptual switching due to ambiguous stimuli [13].

3.3 Expected Performance

Performance analysis of the visual system is based on the assumption that delay and optical resolution are the most important parameters for optimizing system quality. Other important parameters are visual contrast and dynamic range which, however, were not in the focus of the present research.

By using the fundamental relationship G / B = (g/f – 1) ≈ g / f , with f = focal length = 12.5 mm, g = object distance, G = object size, B = image size, and a CCD pixel size of p = 7.5 μm (+ 0.5 μm gap), the vertical

object size at g = 1 km distance corresponding to 1 Pixel is G / B = 0.6 m / 1 Pixel vertical, or ca. 2 arcmin angular resolution, and 1 m / 1 Pixel along the line of sight. The observable resolution at the videopanorama HMI is reduced due to imperfect optics of the camera, the dynamic (illumination dependent) image compression, and resolution of the display system. The optimistic resolution value of about 2' (two times the diffraction limited value of the human eye) may be approached with decreasing camera aperture, which is of course possible only under good light conditions and object – background contrast. For realization of the panorama only 1424x1066 Pixels of each camera (50° viewing angle) are actually used in order to match the 180° panorama angle.

With the known size and distances of static objects on the airfield it is possible to evaluate the practically achieved effective video panorama resolution as compared to the theoretical estimate of 2 arcmin. For verification we used the red-white (1 m squares) multilateration sensor-containers at the end points of the fiber-optic data network as reference objects (see Fig.3, height and width G = 2 m). The nearest containers as captured by the NE and E-looking camera $P_{3,4}$ are located at distances g_E = 400.8 m (Ref.-Obj. 1) and g_{NE} = 588 m (dark blue circle, Ref. Obj. 2) respectively. With the above mentioned lens equation we obtain 7.8 and 5.3 pixels respectively of the camera chip covered by the container images in the vertical direction. These values correspond to a measured resolution of α_V^{exp} = 1.7 arcmin for Ref.Obj. 1 and α_V^{exp} = 1.4 arcmin for Ref.Obj. 2 [14], which appears reasonably close to the theoretical estimate.

The theoretical angular resolution of the PTZ-camera is given by $\alpha_Z = p_H / Z f_0$, yielding α_Z = 1 arcmin (Z = 4, viewing angle 2Θ = 15°) and α_Z = 0.2 arcmin (Z = 23, viewing angle 2Θ = 2.5°), with p_H = horizontal pixel size = 4.4 μm and f_0 (Z = 1) = 3.6 mm.

4. FIELD TESTING

In this section we review the results obtained by flight testing for determining the subjectively experienced visual resolution of the reconstructed far view. The main question to be answered refers to the comparability of the video panorama with the real view out of the tower windows with regard to the control tasks of the operators. For validation of the videopanorama system usability including the zoom function a flight-test plan was set up for experts and non-experts to evaluate identical scenarios under real view and video panorama conditions. Here we report on two experiments performed in 2007 on May 21 with clear sky and 22 with reduced visibility (< 10 km).

4.1 Experimental Design

Flight tests of two hour duration each, with the DLR DO-228 (D-CODE) test aircraft were designed with

successions of approach, touch-and-go (or low approach) and takeoff. Five subjects (2 controllers of the Braunschweig Tower (S_1,S_2) and 3 non-experts (S_3, S_4, S_5, members of the human factors department)) observed the flyby from a position near the panorama camera system and monitored times of 11 characteristic events $e_1 - e_{11}$: out of sight, low / steep dept. angle, take-off, touchdown, approach main / grass runway, landing gear down / up, steep approach, first sighting. The measurements were performed with notebook (touch input) computers by each subject using a specially designed data input software (GUI). Pilots received the flight plan for up to 16 approaches. For the trials a LAN with time synchronized camera and data acquisition touch-input laptops was used. One of the GPS trajectories recorded for each flight with the onboard Omnistar satellite navigation system is shown in Fig.5, including event observation positions $x(e_i)$ of the corresponding observation times $t(e_i)$.

For the present task of determining the perceived video resolution only the four well defined events with the lowest time variances were used (see Table 1).
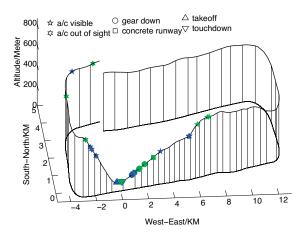

Fig. 5: GPS trajectory no. 4 out of 11 test flights of pre-testing at 13/12/06 (clockwise direction). Open / filled symbols represent event observations under real view / video panorama conditions. Approach direction 260° with touchdown near ARP at 0 km (52°19'09" N, 10° 33'22" E). Vertical lines = 10 s intervals on flight trajectory.

The distance between the airport reference point ARP and departure and approach turning points was ca. 4 km and 14 km respectively. Flights were performed under VFR conditions. Each flyby was characterized by 6 parameters, with parameter values statistically mixed: 1. approaching main (concrete) or grass runway; 2. approach angle normal or high; 3. landing gear out: early, normal, late; 4. low level crossing of airport or touch and go; 5. touch down point early or late; 6. departure angle normal, low angle, steep angle.

While pilots had a detailed plan to follow for the sequence of approaches with different parameter values, the subjects only knew about the different possibilities (e.g. approach grass or main runway)

within the approaches. They had to activate the corresponding field of their input display of the tablet PC and set a time mark at the time of their observation of one out of the 11 possible events during each of the D-CODE approaches / flybys (e.g. a/c visible = first sighting of aircraft under the given (weather) conditions). Also all approaches of additional (non-D-CODE) a/c were monitored. Experts and non-experts were briefed separately before the first experiment, with both groups filling separate questionaires.

4.2 Results and Discussion : Videopanorama

For each trial raw data from all subjects and for all approaches under real view conditions were collected into a single data file. Evaluation of the different approach, touch-and-go, and departure conditions yields the inter-subject time measurement scattering with mean and standard deviation (stdev) of the sample and standard errors (sterr) of mean for the n = 5 subjects [2][14].

Detailed information on the difference between real view and video panorama are obtained by repeating the experiments with the video panorama replay after a week or more in order for the subjects to no longer remember the different flight conditions. It was expected that due to lower resolution of the videopanorama (theoretical estimate $\alpha_V \approx 2$ arc min, see section 3) as compared to the real view, distant events of approaching /departing a/c (like first / last sighting of a/c) should receive an earlier/later mark under real view as compared to video observation. Correspondingly within-subject evaluations of the direct viewing and video panorama replay observations yields time differences t(real view, e_i) – t(video, e_i) < 0 and > 0 for approaching (app) and departing (dpt) a/c respectively.

Results of the initial trial #1 were reported in [2][14], showing experimental visual resolution between 1.3 and 2 arc min, already in reasonable agreement with the theoretical prediction and with the verification measurements (see sect. 3.3). In Table 1 the results for four of the 11 possible observation types are shown for the trials #2, 3 (May 21, sunny day & 22/07, cloudy day), for all subjects and all those flights with pairs of observation (time marks) of real view – video, with no. of observation pairs N, mean Δt(real view - video), standard deviation and std. error of mean.

All displayed events exhibit reproducible and significant pos.(dpt.) and neg.(app.) delays between video panorama and real view conditions. For example the significant negative delay measured as overall mean for e_8 (landing gear visible, -13.0 ± 2.0 s and -13.2± 1.2 s respectively) shows this event to be observable with video only 0.7 km closer to the airport (a/c speed ca. 100 kn = 185 km/h), as compared to the real view conditions (e.g. e_{11}(real view): a/c (lights) recognized at ca. 8 km). If we assume that detection

time difference is determined by the difference of optical resolution between real view (resolution of the human eye ca. $\alpha_E \approx 1$ arcmin = 1/60 °) and videopanorama system, the measured time difference Δt(real view-video) = $t_E - t_V$ from table 2 can be used for calculating the effective resolution α_V of the optical system.

Table 1: Trial #2(May 21/07, clear view > 10 km) and #3(May22/07, cloudy, < 10 km). Mean, standard deviation and std. error of event observation time difference Δt = t(real view)–t(replay).

Trial #2 (clear) Event e_i	N	Mean Δt / s	S.D. / s	S.E. / s
e_{11}: A/C visible	54	-85.1	77.9	10.7
e_8: Gear visible	42	-13.0	12.9	2.0
e_5: touchdown	22	+1.8	1.0	0.2
e_4: Takeoff	17	+2.3	2.5	0.6
Trial #3(cloudy) Event e_i	N	Mean Δt / s	S.D. / s	S.E. / s
e_{11}: A/C visible	54	-26.5	18.3	2.5
e_8: Gear visible	44	-13.2	7.6	1.2
e_5: touchdown	25	+2.0	1.0	0.2
e_4: Takeoff	23	+2.0	1.4	0.3

For suitable events with known object size the single Δt-values allow for calculation of α_V via:

$$\alpha_V = \alpha_E \left(1 + \alpha_E v_E \Delta t / G\right)^{-1} \qquad (1)$$

where the resolution angle α is given by $\alpha_{E,V}$ = G / $x_{E,V}$ measured in rad, with event observation distance $x_{E,V}$ under real view (E) and video replay (V) conditions. G is the object size, e.g. aircraft cross section for e_{11} or landing gear wheel size for e_8. For e_8 we obtain in this way $\alpha_V = 1.4 \, \alpha_E$ (with G(main wheel) = 0.65 m, v_E = 100 kn). For e_{11} (using G(cabin) = 1.8 m) trial #3 yields 1.3 α_E. Both values are in agreement within the experimental uncertainty, although smaller (even better) than the theoretical estimate.

The extremely large observation time difference and s.d. of e_{11} in trial #2 is due to real view event registration under clear view conditions (mostly expert subjects S1, S2) long before the a/c turned towards approach at the ILS turning point. In order to obtain a statistically relevant and model based mean value, a linear regression procedure is employed for those events where the optical resolution (more or less modified by image contrast) may be assumed to play the dominant role for event timing. Because e_1 was unreliable due to observability problems (the aircraft quite often vanished from the P1-camera observation

angle before e_1 was observable), only e_4, e_5, e_8, e_{11} were used for this evaluation. For applying a regression procedure the independent variable "event e_i" has to be replaced by a quantifiable variable. A linear model is obtained when considering the observation distance x as obtained from the GPS reference trajectory instead of the observation time, yielding the $\Delta x(E - V) = v_E(t) \, \Delta t$ versus x_E dependence for regression analysis as depicted in Fig. 6 for trial #3 (cloudy day).
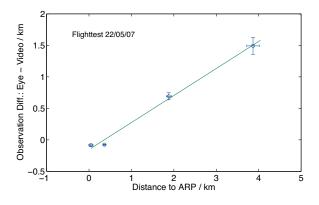

Fig. 6: Mean event-observation position differences Δx (real view – video replay) between real far view and video panorama conditions versus mean GPS-position estimate of x_E (= distance from event position x_E to airport reference point ARP) for trial #3. Error bars represent S.E. of means. Straight line: linear regression.

The scatter plot of the four data points ([x_E, $\Delta x = v_E \Delta t$], for e_4, e_5, e_8, e_{11}) is obtained by correlating the measured time values with the corresponding GPS position data.

For data fitting the theoretical relationship

$$\Delta x\left(\text{eye} - \text{video}\right) = \left(1 - \alpha_E/\alpha_V\right) x_E \qquad (2)$$

$$\alpha_V = \alpha_E \left(1 - \beta_1\right)^{-1} \qquad (3)$$

is employed. With the slope $\beta_1 = \Delta x/x_E$ = 0.429 (± 0.02 std.err., R^2 = 0.99, significance level F = 321 at p = 0.003) the corresponding α_V estimate of 1.75 arcmin (±0.08) is obtained, exhibiting even better agreement with the predictions of section 3.4 than the initial trial#1, reported in [14].

4.3 Results and Discussion: Zoom Function

In order to decrease the duration of the replay experiments for evaluating observations with the PTZ camera (e11, e8) only the approach sections of the videos until touchdown (event e_5) were used. Because due to this procedure time synchronization with real-view experiments was lost, PTZ experiments were related to panorama replay with touchdown time as common reference. For data evaluation equation (1) with substitution of α_V through α_{PTZ} and α_E through a_V was used, yielding

$$\alpha_{PTZ} = \alpha_V \left(1 + \alpha_V v\Delta t/G\right)^{-1} \qquad (4)$$

The experimental results for the effective PTZ resolution yield mean values $\alpha_{PTZ} = 1.2 - 1.3$ arcmin for zoom factor $Z = 3.6 - 4$, obtained from 84 observations of events e_{11} and 24 observations of e_8.

They are reasonably close to the theoretical value $\alpha_{PTZ} \approx 1' = \alpha_E$ as obtained under the hypothesis of resolution limited object detection times. These data were obtained with 20 subjects observing those three rounds around the airport on each of the two days, which included a touchdown (e_5) to be used as common PTZ – videopanorama reference with Δt (Panorama – PTZ) ≈ 0 s.

5. RTC-SIMULATION ENVIRONMENTS

The design and development of the new Remote Tower Center work environment is supported by tower simulator based and microworld computer simulations which are controlled by formal process and decision models.

5.1 Airport Microworld Computer Simulation

In previously reported work [6] the formalised results of an airport tower work and task analysis provided the input data for a Formal Airport Control Model (FAirControl) for the simulation of the controller decision making processes at the tower work positions. In [8][9] it is shown how the results of a cognitive work analysis are transferred into an executable human machine model, based on Colored Petri Nets (CPN) [10] as graph theoretical tool for simulating the controllers work processes in relation to the airport processes.

The formal model allows for evaluation of different alternatives of work organization under simplified but reproducible laboratory conditions. It also supports the design of the new work environment and the monitoring of psychological parameters, e.g. uncovering of reduced situational awareness. The model is separated into submodels for the human agent (controller), human system interaction, and the traffic process [6][8][9]. The corresponding highest hierarchy CPN level is shown in Fig.7.

Rectangles represent substitution transitions between places (ellipses) as system states representing three subnets for (from left to right) the airport traffic process, the human-system interaction, and the decision making of the cognitive agent (controller) on the lower CPN-hierarchy levels. Ellipses represent the places for tokens which dynamically move througout the net structure via activated (firing) transitions, and together with the transitions they constitute the static structure of the system. In Fig.7 they represent the process tasks, events and the human ressources (three places at the right), which are connected via the interaction substitution-transition with the input/output

states and the airport ressources (three places at the left).

The state of the airport process model (Fig.8) determines the type and content of visual and electronic surface traffic information (e.g. usage of taxiways, landing clearance) which can be acquired and communicated by the controller.

The V-shaped sequence of places and (replacement) transitions represent (from left to right) the corresponding timed process sequence from approach via taxi-in, apron/parking (block), pushback, taxi-out, takeoff, airbound.
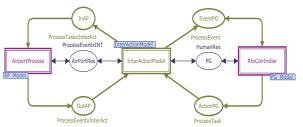

Fig. 7. Controlled airport system as Human Machine System is mapped on the highest hierarchy level of a Colored Petri Net. Transitions (rectangles) between places as system states (ellipses) include subnets for airport process, interaction model, and controller model (from left to right).

The interaction model includes sub networks for description of information resources, such as radio communication and visual perception of the traffic situation. Consequently the human model(s) and machine model(s) can work independently from each other for certain time periods.
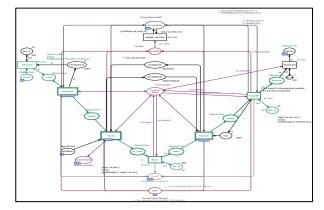

Fig. 8. Subnet for the airport process, including lower level subnets for approach, taxi-in, taxi-out processes.

The controller model (human model) is implemented as a Formal Cognitive Resource (FCR) Model [7][9] and serves for the description of controller behaviour in the tower work environment. In the present version it is reduced to a completely rule based process. The task execution process on the 3rd CPN hierarchy sublevel (as subnet of the controller model on the 2nd level, not shown) is depicted in Fig. 9.

Controller's decisions, e.g. "deliver startup clearance" are substitution transitions (rectangles) representing decision subnets on the lowest hierarchy level. Places (ellipses) at the left and right of the figure represent

goal states / process states / human ressources and actions / events respectively.

The CPN-controlled airport human machine system drives a schematic microworld visualisation via TCP/IP based communication between the Petri net (Fig. 7) and the visualization , programmed in C++ (depicted in Fig. 10). Active communication between pilot and controller during task execution is highlighted by different coloring of the labeling of the symbolized aircraft moving within the microworld visualization.
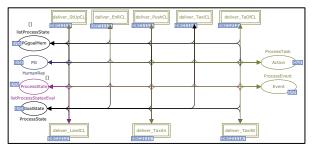

Fig. 9: Controllers tasks which are implemented in the mental model of the agents on the third subnet level.

The formal work process model with graphical representation of the controlled traffic process improves the communication between domain experts and system developers by simulating different traffic situations to establish a basis for a structured interview of those situations. Interviews of two senior controllers focused on the visual information from the outside view. They provided input for the model development [6][8].
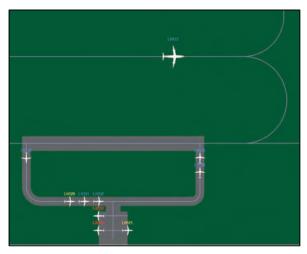

Fig 10: FairControl Airport microworld: Graphical visualization of the simulated controlled inbound/outbound sequence of a generic small airport.

The present FairControl version with one controller managing the microworld airport traffic [21] (see Fig.7, in contrast to [8] with two interacting controllers) serves for validating certain implemented aspects of the rule based Petri net agents decision making and task execution, e.g. selection of alternative strategies [16]. For this purpose the agent can be turned off and the microworld traffic can be controlled by human

operators by communication with the airport process via the interaction module. The interaction of the human operators with the CPN controlled traffic process is monitored and the attention/perception can be measured via eye-tracking [16].

For simulating the simultaneous control of two airports from a remote tower center (RTC) the existing FAirControl microworld is presently being extended accordingly by adding a second airport process and a second controller agent. It will provide the possibility to investigate work distribution and performance of cooperating controllers in a simplified RTC microworld environment under different laboratory conditions of work organisation and for different traffic scenarios. It also supports the monitoring of psychological parameters, e.g. uncovering of reduced situational awareness.

5.2 Airport Tower Center Simulator

For investigating possible RTC work system alternatives with different traffic scenarios, DLR's Apron and Tower simulator (ATS) was extended by a remote tower operator console as shown in the photo of Fig. 11.

Fig. 11: RTC simulator environment. Photo of the 200° vision system of DLR tower simulator (ATS) with extension by the 180°-RTO console, showing live Panorama. Photo: DLR.

The main purpose of the RTO console is to provide a live panorama display of the Braunschweig airport traffic situation including PTZ camera, displayed on the touch input display which is integrated into the console (see also Fig.3). Alternatively the console is presently prepared for optionally switching into simulator mode for displaying a second simulated airport traffic situation within DLR's ATS system, by means of a second image generator and coupling to the traffic simulation engine.

There are several reasons for validating the RTC concept, besides field tests (see sect. 4), also by means of integration into a real-time simulation environment. First of all it ensures control and reproducibility over experimental conditions and constraints. Variation of traffic mix and load, environmental conditions and the creation of possibly conflicting situations allows the evaluation of human factors and safety related issues.

Furthermore, the ability to vary between different controller work position (CWP) configurations and operational procedures in the simulator will enable a more comprehensive analysis of related organisational and operational constraints for the implementation of the new RTC concept. The intended simulation setup supports also the analysis of HMI- and RTC-work system design. The real-time simulation capabilities are intended for validating the two RTC configurations mentioned in section 2:

1) Integrated RTO working position within a real tower environment (e.g. tower cab of larger airport)
2) RTO working positions located within an RTC for ≥ 2 small airports (including variation of single-airport- and multi-airport-CWPs)

Integrated into the simulator, the live traffic source of the RTO console will be replaced by a virtual representation of the outside view, based on traffic movements now generated by a simulation engine. With switching into simulator mode, not only the camera view will be replaced by a panorama derived from an image generator (IG) but also the position data, flight plan data and weather information, and airfield lighting will be provided by the simulation. Thus also the augmented vision capabilities of the RTO CWP are usable and can be examined within the validation setup.

In addition, the setup with two or more RTO consoles (two-airport RTC) connected to ≥ 2 image generators and traffic engines leads to a multiple-airport RTC tower simulation. Both configurations will provide simulated air traffic at two different airports within a combined work environment.

Together with the analysis of the simplified FairControl microworld (lab-type) simulations, the real-time simulator experiments are an integral part of the (cycled) concept development- and validation process. Due to its characteristics, the experiments carried out within the simulator will focus on certain specific issues. The experimental design will cover the analysis of operational procedures, the dedicated work environment and the evaluation of its influences on controller workload and situational awareness. Additionally the developed work share within the combined RTC environment will be observed and analysed as well as attention- and perception related factors. Within the experiments variation of different visual conditions, including reduced visibility conditions (fog) as well as a variation of available light situations (day- and night-time conditions) will be examined.

To ensure the validation environment is as realistic as possible (and necessary), experiences and results from field trials at Braunschweig airport (see sect. 4) can be used for calibration and alignment of the simulator setup based on comparison between recorded traffic data and video signals and simulated air traffic.

Finally, the setup and configuration of field testing equipment, RTO work positions, and simulation environments at the Research Airport Braunschweig also allows for using the implemented RTO CWP under shadow mode conditions for control of air traffic at the BWE airport, i.e. with controllers following the real traffic in parallel to the controller staff in charge, however without interacting with the pilots.

6. SUMMARY AND CONCLUSION

Basic scenarios and elements of DLR's experimental Remote Tower Center (RTC) system at the Braunschweig Research Airport are described. Quantitative evaluation of field trials for comparing real view and video panorama observation verified the theoretically predicted video panorama and PTZ resolution of ca. 2 arcmin and ca. 1 arcmin (with zoom factor $Z \approx 4$) respectively. The latter one corresponds to the foveal resolution of the human eye and exceeds it with increasing Z, approaching the physical diffraction limit. Presently extensions of the augmented vision videopanorama system are under way for improving the low visibility conditions, including high a resolution infrared sensor and a second PTZ camera near the runway. Another improvement concerns the augmented vision function which will be turned into an active visual assistance system by enhanced usage of automatic image processing. As most important extension a second more distant airport will be connected to the present experimental system for evaluating live video data transmission bandwidth limitations and delay, and reliability.

Besides the experimental sensor system and video panorama based HMI a RTC simulator environment is realized. It consists of a tower simulator including a compact remote tower operator (RTO) console, for simulated control of two airports and a simplified microworld computer simulation for reproducible (computer) experiments with different work organisation alternatives.

7. ACKNOWLEDGMENTS

REFERENCES

[1] Schmidt, M., Rudolph, M., Werther, B., Fürstenau, N., "Remote Airport Tower Operation with Augmented Vision Video Panorama HMI", Proc. 2nd Int Conf. Res. in Air Transportation ICRAT, Belgrade (2006) p. 221–230

[2] Schmidt, M., Rudolph, M., Werther, B., Möhlenbrink, C. Fürstenau, N., "Development of

an Augmented Vision Video Panorama Human-Machine Interface for Remote Airport Tower Operation", In: M.J. Smith, G. Salvendy (Eds.) Human Interface II, Lect. Notes Computer Science vol.4558, Springer-Verlag Berlin Heidelberg (2007), p. 1119-1128,

[3] Tavanti, M., "Control Tower Operations: A Literature Review of Task Analysis Studies". EEC Note 05 (2006)

[4] Pinska, E., "An Investigation of the Head-up Time at Tower and Ground Control Positions". Proc. 5th Eurocontrol Innovative Research Workshop (2006) 81-86

[5] K.J. Vicente, "Cognitive Work Analysis", Mahwah/NJ: Lawrence Erlbaum Associates, 1999.

[6] Werther, B., Uhlmann, H., "Ansatz zur modellbasierten Entwicklung eines Lotsenarbeitsplatzes". In: Zustandserkennung und Systemgestaltung, Fortschritt Berichte VDI, 22 (2005) 291 -294.

[7] Werther, B., "Kognitive Modellierung mit farbigen Petrinetzen zur Analyse menschlichen Verhaltens". PhD Dissertation, DLR-Inst. of Flight Guidance, (2006).

[8] Werther, B., "Colored Petri net based modeling of airport control processes". In: Proc. Int. Conf. Comput. Intelligence for Modelling, Control & Automation (CIMCA) Sydney (2006) IEEE ISBN 0-7695-2731-0

[9] Werther, B., Schnieder, E., "Formal Cognitive Resource Model: Modeling of human behavior in complex work environments", in: Proc. Int. Conf. Computational Intelligence for Modelling, Control & Automation (CIMCA 2005), Wien: 2005, pp. 606 – 611.

[10] Jensen, K., "Coloured Petri Nets". Berlin: Springer, 1997.

[11] N. Fürstenau, M. Rudolph, M. Schmidt, B. Lorenz, T. Albrecht, "On the use of transparent rear projection screens to reduce head–down time in the air–traffic control tower", Proc. Human Performance, Situation Awareness and Automation Technology (HAPSA II), Daytona Beach , Lawrence Erlbaum Publishers Inc. (2004), 195–200

[12] Peterson, S., Pinska, E., "Human Performance with simulated Collimation in Transparent Projection Screens". Proc. 2nd Int. Conf. Res. in Air Transportation, Belgrade (2006) 231-237.

[13] Fürstenau, N., "Modelling and Simulation of spontaneous perception switching with ambiguous visual stimuli in augmented vision systems". Lecture Notes in Artificial Intelligence 4021 (2006) Springer-Verlag, Berlin, New York, 20-31

[14] N. Fürstenau, M. Schmidt, M. Rudolph, C. Möhlenbrink, B. Werther, "Development of an Augmented Vision Videopanorama Human-Machine Interface for Remote Airport Tower Operation", in: Proc. 6th Eurocontrol Innovative Res. Workshop, Eurocontrol Experimental Center, Bretigny (2007) 125-132

[15] N. Fürstenau, M. Schmidt, M. Rudolph, C. Möhlenbrink, W. Halle, "Augmented vision videopanorama system for remote airport tower operation", in: Proc. ICAS 2008, 26th Int. Congress of the Aeronautical Sciences. I. Grant (Ed.), Anchorage, (2008) ISBN 0-9533991-9-2

[16] Möhlenbrink, C, PhD Dissertation, to be published

[17] SESAR Definition phase Deliverable 2: "Air Transport Framework: The Performance Target". Document No. DLM-0607-001-02-00 12-2006

[18] Matas, M., "Future Airport Concept", in: Proc. 4th Eurocontrol Innovative Workshop, Dec. 6-8 (2005) 135-150

[19] http://www.dlr.de/fl/en/desktopdefault.aspx/tabid-1149/1737_read-3120/

[20] Ellis, S., "Towards determination of visual requirements for augmented reality displays and virtual environments for the airport tower". Proc. NATO workshop on Virtual Media for the Military, West Point /N.Y., HFM-121/RTG 042 HFM-136, (2006) 31-1-31-9

[21] Werther, B., Möhlenbrink, C., Rudolph, M., "Colored petri net based formal airport control model for simulation and analysis of airport control processes", In: V.G. Duffy (Ed.) Digital Human Modeling, Lect. Notes Computer Science vol.4561, Springer-Verlag Berlin Heidelberg (2007), p. 1027-1036,

COPYRIGHT